Diabetologia (2001) 44: 1054–1061

Diabetologia

Low rate of proliferation in immature thymocytes of the non-obese diabetic mouse maps to the *Idd6* diabetes susceptibility region

M-L. Bergman[1*], C. Penha-Gonçalves[2†], K. Lejon[1], D. Holmberg[1]

[1] Department of Cell and Molecular Biology, Umeå University, Umeå, Sweden
[2] Gulbenkian Institute for Science, Oeiras, Portugal

Abstract

Aims/hypothesis. The non-obese diabetic (NOD) mouse spontaneously develops T-cell-dependent autoimmune diabetes. This mouse strain has a number of immune dysfunctions related to T-cell development but so far there are no available data on the proliferation of NOD immature thymocytes. We therefore studied the thymocyte proliferation in the NOD mouse in discrete stages of T-cell development.
Methods. We depleted thymocytes in vivo and analysed thymocyte proliferation during the thymus recovery from depletion. We used co-segregation analysis and quantitative loci trait analysis to investigate the genetic control of proliferation impairments in NOD thymocytes.
Results. Immature thymocytes of female NOD mice proliferate with a relatively low rate compared to non-autoimmune C57Bl/6 mice. This aberrant proliferation was most pronounced in $CD4^{-/lo}$ $CD8^{+}$ cells differentiating from the $CD4^{-}CD8^{-}$ to the $CD4^{+}CD8^{+}$ stage. A genetic mapping study using an F2 intercross between the NOD and the C57BL/6 strains showed that a major locus controlling this trait is linked to the insulin-dependent diabetes susceptibility locus *Idd6*.
Conclusion/interpretation. Our results suggest that impairment of proliferation of immature thymocytes is one possible mechanism through which the Idd6 locus contributes to the pathogenesis of diabetes. [Diabetologia (2001) 44: 1054–1061]

Keywords NOD, immature thymocytes, proliferation, genetics.

Non-obese diabetic (NOD) mice spontaneously develop autoimmune diabetes, a disease that closely resembles Type I (insulin-dependent) diabetes mellitus in humans [1]. This T-cell-dependent autoimmune disease is multifactorial and polygenic, with at least 18 separate loci involved in the disease process in the NOD mouse [2–5]. The genetic factors represented by these loci have not yet been identified, although MHC class II genes are strong candidates for the *Idd1* locus [6]. In search for the genes that control diabetes we have taken the approach of identifying and genetically mapping NOD-specific traits that are related to lymphocyte physiology.

A number of immune dysfunctions of the NOD mouse are related to thymocyte development and thymic homeostasis. Thus, defective apoptosis induction has been identified in NOD thymocytes after Dexamethazone (DXM) treatment [7] and after γ-irradiation [8]. These defects were shown to be controlled by loci mapping within the *Idd6* [9] and the *Idd5* [8] regions, respectively. Unresponsiveness of mature NOD thymocytes to ConA stimulation has also been reported [10] and genetically mapped to the *Idd4* region [11].

Received: 6 November 2000 and in revised form: 3 May 2001

Corresponding author: D. Holmberg, Department of Cell and Molecular Biology, Umeå University, S-901 87 Umeå, Sweden
Abbreviations: NOD, non obese diabetic mice; Idd, insulin-dependent diabetes locus; DXM, dexamethazone; PFA, paraformaldehyde; DN, $CD4^{-}CD8^{+}$, DP, $CD4^{+}CD8^{+}$; BrdU, 5-bromo-2'-deoxy-uridine; QTL, quantitative trait loci; TCR, T-cell receptor; LOD, log-likelihood of the odds

* These two authors have contributed equally to the work

Thymocyte development proceeds through an ordered sequence of developmental stages [12, 13]. Progression of individual cells through the developmental pathway is dependent on scrutiny in selective checkpoints that results either in cell death or in cell survival. A proliferation phase precedes each of these developmental checkpoints and leads to an expansion of cells that will be exposed to selection.

The first proliferation phase is detected in the early immature double negative, $CD4^-CD8^-$ (DN) thymocytes [14]. Within this compartment the cells evolve through a series of stages leading to the expression of the $CD44^-CD25^+$ phenotype [15]. This subset of DN thymocytes enters a phase of growth arrest that is thought to correspond to a selection step based on the expression of the TCR β chain on the cell surface – a process called β selection [16].

After β selection, a second expansion phase occurs along with the differentiation from the $CD4^-CD8^-$ (DN) to the $CD4^+CD8^+$ (DP) stage. The cells that have rearranged a functional TCR β chain enter active cell cycling and undergo rearrangement of the α chain locus. Analysis of proliferating adult [14] and TCR β + fetal thymocytes [17] estimate that after β selection, one thymocyte can undergo up to nine cell divisions, corresponding to a 300-fold cell expansion. This phase of proliferation occurs in the intermediate $CD4^- 8^+$ and $CD4^{lo}8^+$ populations and in the DP compartment [14, 18]. The $CD4^{-/lo}$ $CD8^+$ intermediates are minor thymocyte populations that represent a differentiation stage in the DN-DP transition where proliferation is intense. The expansion of these cells is thought to increase the number of individual TCR-β chains that are available to associate with the newly rearranged α-chains.

Thereafter, the DP immature thymocytes undergo a stringent process of selection based on the functionality and specificity of the $\alpha\beta$ TCR, in the course of which the vast majority of this population dies by apoptosis [19]. This cell loss is counterbalanced by cell proliferation and it is estimated that the DP compartment is replenished with new cells approximately every 3.5 days in a 2 month-old mouse [20]. Hence, DP cellularity is maintained by compensating cell death with cell proliferation occurring both in the $CD4^{-/lo}$ $CD8^+$ intermediate cell populations and in the DP compartment.

The second phase of cell proliferation accomplishes the double task of expanding the number of cells that have successfully rearranged the TCR β-chain gene and replenishing the highly dynamic DP compartment. Therefore, the proliferative functions are crucial to guarantee the thymic homeostasis and could influence the development of the T-cell repertoire.

So far, there are no available data on cell proliferation during the early stages of T-cell development in the NOD mouse. We have analysed the replenishment of the DP compartment in the NOD thymus from more immature cells and report on the genetic control of proliferation impairments in the immature thymocyte compartments of the NOD mouse.

Materials and methods

Mice. Non-obese diabetic (NOD), C57BL/6, F1(NOD x C57BL/6) and F2(NOD x C57BL/6) mice were bred and kept in conventional facilities at Umeå University. All mice used were females between 7 and 8 weeks of age. The incidence of diabetes among the females of the NOD colony is 70% by 6 months of age. The principles of laboratory animal care (NIH publication 85–23, revised 1985) and the Swedish national guidelines for animal research were followed.

Depletion of DP thymocytes. To severely deplete DP thymocytes, the mice were injected i.p. with 0.5 mg DXM (Merck Sharp Dome). The mice were killed on day 3 to day 6 after treatment. Thymi were harvested and single cell suspensions were prepared by gently forcing the cells through a nylon filter.

Thymocyte analysis. Thymocytes were counted using an electronic cell counter (Coulter counter). For analysis of proliferation of thymocyte sub-populations, mice were injected i.p. with 1 mg of BrdU (5-Bromo-2'-deoxy-uridine; Sigma-Aldrich, St Louis, Mo., USA) in PBS (5 mg/ml) 3 hours before they were killed. A combined staining for surface molecules and incorporated BrdU was used adapting a protocol by others (21). After conventional surface staining with anti-CD4-Phycoerythrin, anti-CD8-biotin (Becton and Dickinson, Franklin Lakes, N.J., USA) and streptavidin-Cy-chrome (Becton and Dickinson), cells were washed once, resuspended in 0.15 mol/l NaCl, and fixed by dropwise addition of cold 95% ethanol up to 70%. Then the cells were incubated for 30 min, washed in PBS, and treated overnight at 4°C with 1% PFA, 0.01% Tween 20. The cells were pelleted, incubated with 40 Kunitz units of DNase I (Sigma) in 0,15 mol/l NaCl, 4.2 mmol/l $MgCl_2$ (pH 5) for 20 min (37°C), washed once and stained with mouse anti-BrdU (Sigma) antibody for 30 min. The cells were washed twice, and incubated for 30 min with anti-mouse Ig FITC antibody (Becton and Dickinson). Non-BrdU injected mice were used as negative controls for BrdU incorporation. After staining, the cells were analysed in a FACScalibur cytometer using Cell Quest software (Becton and Dickinson). The number of cells of the different thymocyte sub-populations was calculated by multiplying the total number of counted cells by the fraction represented by the sub-population out of all thymocytes as analysed by FACS.

Genotyping. To genotype the F2 (NOD x C57BL/6) progeny we used markers that identify DNA single sequence tandem repeat polymorphisms between the parental NOD and C57BL/6 strains. The F2(NOD x C57BL/6) mice were genotyped for markers mapping on chromosomes 1, 3, 4, 6, 7, 9, 11, 14 and 17. Marker DNA was amplified using primers purchased from Research Genetics (Huntsville, Ala., USA). The primers for IL2 and plau markers were synthesized as described [22]. One marker mapping within each of the *Idd* regions that are known to segregate in this cross (*Idd1-10, 16, 17* and *18*) was used for an initial screening of genetic association. Additional markers were used to analyse the regions to which association was suggested. Amplifications from tail DNA were optimized for each microsatellite, varying the annealing

Table 1. Thymocyte recovery after DXM treatment

Days after DXM	C57BL/6	NOD	F1(C57BL/6XNOD)	NOD recovery efficiency	*t*-test (*p* value)
3	16.4 (± 1.5)	15.1 (± 1.4)	13.8 (± 1.0)	0.93	0.11
4	22.3 (± 3.9)	17.1 (± 6.0)	18.0 (± 1.0)	0.78	0.072
5	52.2 (± 9.3)	37.1 (± 3.1)	43.5 (± 6.8)	0.71	0.0097
6	66.8 (15.4)	54.4 (± 3.4)	52.7 (± 17.8)	0.85	0.017

The number of total thymocytes ($\cdot 10^6$) is indicated and represents the average of 4 to 5 mice (standard deviations are given in parentheses). Nod recovery efficiency was calculated as a ratio between the NOD average and C57BL/6 average at each time point. The *p* values represent results of *t*-tests comparing the group of NOD females with the C57BL/6 females at each time point

Table 2. Double Positive thymocytes recovery after DXM treatment

Days after DXM	C57BL/6	NOD	F1(C57BL/6XNOD)	NOD recovery efficiency	*t*-test (*p*)
3	0.9 (± 0.4)	0.9 (± 0.1)	1.0 (± 0.3)	1.07	0.37
4	7.7 (± 1.8)	5.4 (± 2.7)	6.9 (± 2.1)	0.71	0.076
5	41.6 (± 7.9)	26.8 (± 3.0)	34.6 (± 7.8)	0.67	0.0060
6	54.5 (± 14.5)	44.5 (± 3.8)	44.0 (± 14.8)	0.86	0.19

The number of $CD4^+CD8^+$ cells ($\cdot 10^6$) is indicated and represents the average of 4 to 5 mice (standard deviations are given in parentheses). NOD recovery efficiency and *p* values were calculated as for Table 1

temperature (53–57 °C). Amplified fragments were analysed in 4 % agarose gels (3 % NuSieve GTG agarose + 1 % type II agarose; Sigma) stained with ethidium bromide. Genetic markers used in this study included: D1MIT21, D3MIT51, IL-2, D4MIT72, D6MIT304, D6MIT15, D6MIT14, D6MIT57, D6MIT198, D6MIT194, D6MIT218, D6MIT64, D6MIT9, D6MIT184, D7MIT76, D7MIT55, D7MIT270, D7MIT145, D9MIT9, D11MIT39, PLAU, D17Mit28.

Statistics. To evaluate differences between groups of animals we did a Student's *t*-test for two-sample unequal variance groups (heteroscedastic) and the *p*-values for one-tailed distributions are shown. A *p* value of less than 0.01 was considered to be statistically significant.

Genetic analysis. For each genotyped marker, the association to the proliferation phenotype was analysed in contingency Tables by a chi square test. Marker order and recombination fractions were calculated with multi point analysis using Mapmaker 3.0/Exp. software [23]. Quantitative Trait Loci (QTL) were analysed using the Mapmaker/QTL software [24].

Results

Slow cell recovery of NOD thymocytes after DP depletion. To study the ability of NOD thymocytes to proliferate in vivo, we depleted DP immature thymocytes by in vivo treatment with DXM and we followed the kinetics of cell recovery in the thymus. We have previously shown that intra-peritoneal injection of 0.2 mg DXM/mouse leads to a severe depletion of DP thymocytes in C57BL/6 mice while at this dose NOD thymocytes are relatively resistant [7]. At a dose of 0.5 mg DXM/mouse, however, a similar degree of cell depletion in C57BL/6 and NOD female mice is observed with a maximum depletion of DP thymocytes observed 3 days after treatment (Table 1). The kinetics of cell recovery from day 3 to day 6 after treatment showed that the number of cells in the NOD thymus was recovered with a slower rate compared to the C57BL/6 control mouse strain. The effect of this difference became most pronounced at recovery day 5 and was evident both for the recovery of total thymocytes (Table 1) and of DP cells (Table 2). The thymocytes are heavily depleted in the recovering thymus and the relative sizes of thymocyte compartments are altered. Taking this into account, the differences in cell numbers observed at recovery day 5 represent a considerable difference in the efficiency of recovery. In fact, the total cell recovery in NOD mice at day 5 represents only 71 % of the recovery achieved by the C57BL/6 mice and the recovery efficiency of NOD DP cells is 67 % (Tables 1, 2). A similar recovery difference was observed in an independent kinetic experiment that tested 3 NOD females and 3 C57BL/6 females at each time point. At day 5 the cellularity in the NOD thymus was $32.0 \cdot 10^6$ (± 15.1) total thymocytes and $26.9 \cdot 10^6$ (± 13.2) DP cells while in the C57BL/6 thymus was $43.3 \cdot 10^6$ (± 11.6) and $35.2 \cdot 10^6$ (± 11.8), respectively. Again, these differences represent a considerable deficit of recovery efficiency by the NOD thymus (approximately 75 %). We concluded that the observed differences in thymic cellularity between NOD and C57BL/6 at day 5 are genuine because they were considerably large, reproducible and statistically significant (Tables 1 and 2).

Low rate of proliferation of NOD immature thymocytes. To search for the origin of these deviations in

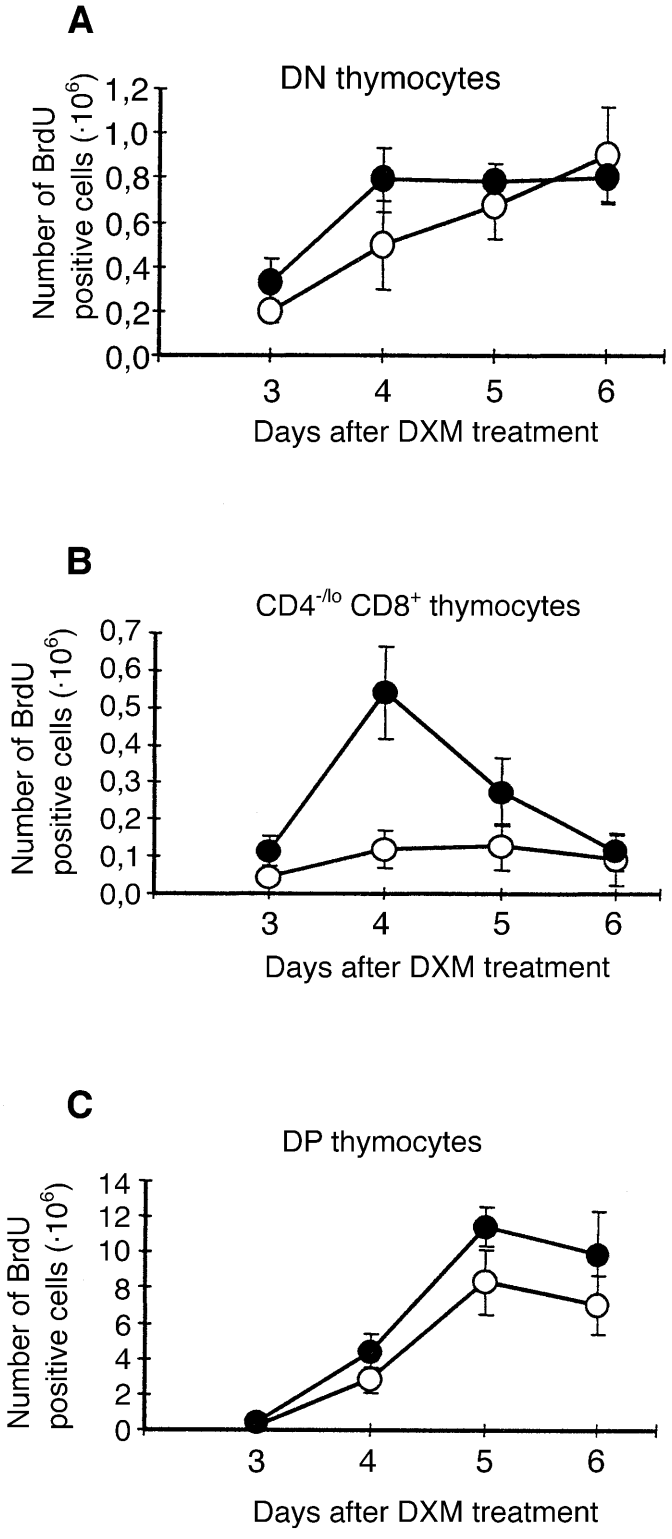

Fig. 1, A–C. Kinetics of thymocyte proliferation after DXM induced depletion. Thymocytes from NOD female mice (○) and C57BL/6 female mice (●) treated with DXM and injected with BrdU were collected, counted and stained with anti-CD4, anti-CD8 and anti-BrdU antibodies. The plots show the number of **A** $CD4^-$ $CD8^-$, **B** $CD4^{-/lo}$ $CD8^+$ and **C** $CD4^+$ $CD8^+$ cells incorporating BrdU. Data points and error bars represent the average values and the standard deviations of 3–5 mice. A Student's *t* test confirms that the difference in $CD4^{-/lo}CD8^+$ cells observed at day 4 **B** is statistical significant ($p < 0.002$)

the recovering NOD thymus, we analysed cell proliferation in different thymocyte sub-populations by pulse labelling in vivo with a DNA precursor (BrdU). A time-course experiment showed that the number of proliferating cells detected within the DN T-cell population was lower in the NOD than in C57BL/6 female mice (Fig. 1A). The observed difference in the number of proliferating cells was most striking within the intermediate population $CD4^{-/lo}$ $CD8^+$. This population displays a peak in proliferation at day 4 in C57BL/6 mice that is absent in the NOD mice (Fig. 1B). This proliferation difference at day 4 was reflected in the size of the $CD4^{-/lo}$ $CD8^+$ population which was larger in C57BL/6 mice ($5.1 \cdot 10^6 \pm 0.49$) as compared to NOD mice ($3.3 \cdot 10^6 \pm 1.1$). The absence of a proliferation peak in the NOD $CD4^{-/lo}$ $CD8^+$ population at day 4 was also observed in an independent experiment using 13 NOD females that had an average of $0.6 \cdot 10^6$ (± 0.34) $CD4^{-/lo}$ $CD8^+$ proliferating cells while ten C57BL/6 females had $3.2 \cdot 10^6$ (± 1.0). This difference was shown to be statistically significant in a Student's *t*-test ($p < 0.00001$). These two independent experiments both revealed a five-fold deficit of the number of proliferating CD4-/lo CD8 + cells at day 4 in the NOD thymus. This thymocyte subset is believed to be the immediate derivative of the DN population and to precede the DP thymocytes. A less pronounced difference in the number of proliferating cells was observed in DP thymocytes, reaching a maximum on day 5 after treatment (Fig. 1C). Thus, one day after the observed difference in proliferation of the generative $CD4^{-/lo}$ $CD8^+$ population, the difference in cellularity within the DP compartment reaches a maximum. These observations correspond with the difference in total cellularity evident mainly in the DP compartment (Table 2). Together, these data suggest that the origin of the deficit in total cellularity in the recovering NOD thymus primarily results from an impairment in the proliferation of the $CD4^{-/lo}$ $CD8^+$ population (Fig. 2). This impairment does not seem to be sex- or age-dependent as we have observed a similar proliferation phenotype in NOD males at 7 to 8 weeks of age and in NOD females at 4 weeks of age (data not shown)

The CD4-/lo CD8 + proliferation trait in F2(C57BL/6 x NOD) mice. To study the genetic control of the impairment observed in the $CD4^{-/lo}$ $CD8^+$ population of the NOD mouse, we analysed the DNA synthesis in the thymocytes of a F2(C57BL/6 x NOD) female progeny 4 days after DXM treatment. In each of the 87 F2 female mice we measured the proportion of $CD4^{-/lo}$ $CD8^+$ cells out of the thymocytes incorporating BrdU – the $CD4^{-/lo}$ $CD8^+$ proliferation trait. This trait was normally distributed in the F2 progeny and showed an average value between the two parental strains. The phenotypic variance spans from low trait

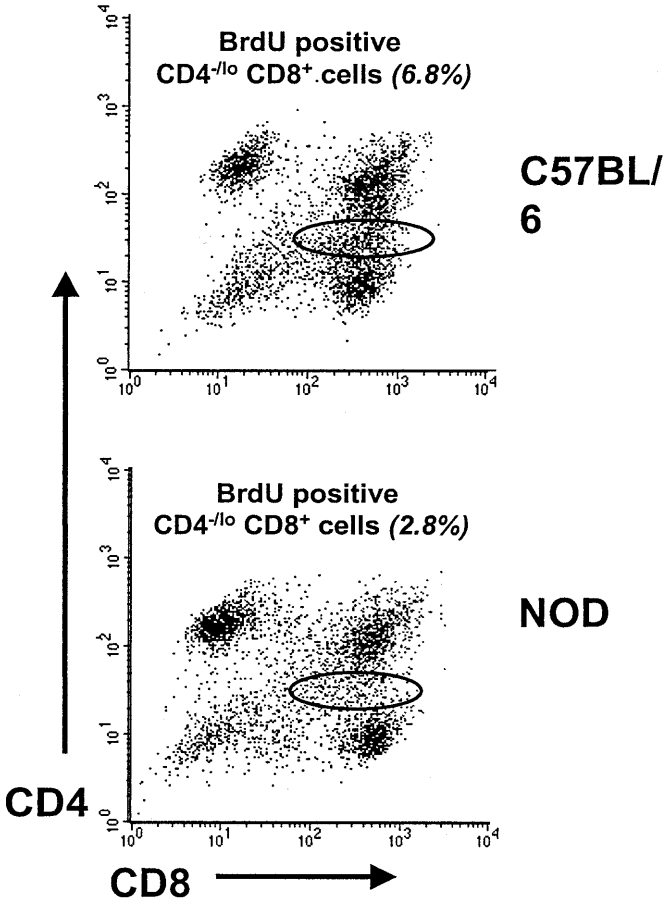

Fig. 2. Impaired proliferation of $CD4^{-/lo}$ $CD8^+$ NOD thymocytes. Dot plots represent thymocytes from C57BL/6 and NOD female mice stained with anti-CD4-PE, CD8-Cy and with anti-BrdU (indirectly labelled with FITC) antibodies. The thymocytes were collected 4 days after DXM injection and 3 h after BrdU injection. Circles identify the $CD4^{-/lo}$ $CD8^+$ population and the percentages represent the percent of $CD4^{-/lo}$ $CD8^+$ $BrdU^+$ cells out of the BrdU incorporating thymocytes. The plots are representative of results obtained from 10 C57BL/6 (7.4 % ± 1.2) and 14 NOD (3.3 % ± 1.1) female mice. The BrdU positive cells are represented as red dots accounting for 30 % (± 3.2) and 16 % (± 7.5) of the total thymocytes in C57BL/6 and in NOD mice, respectively

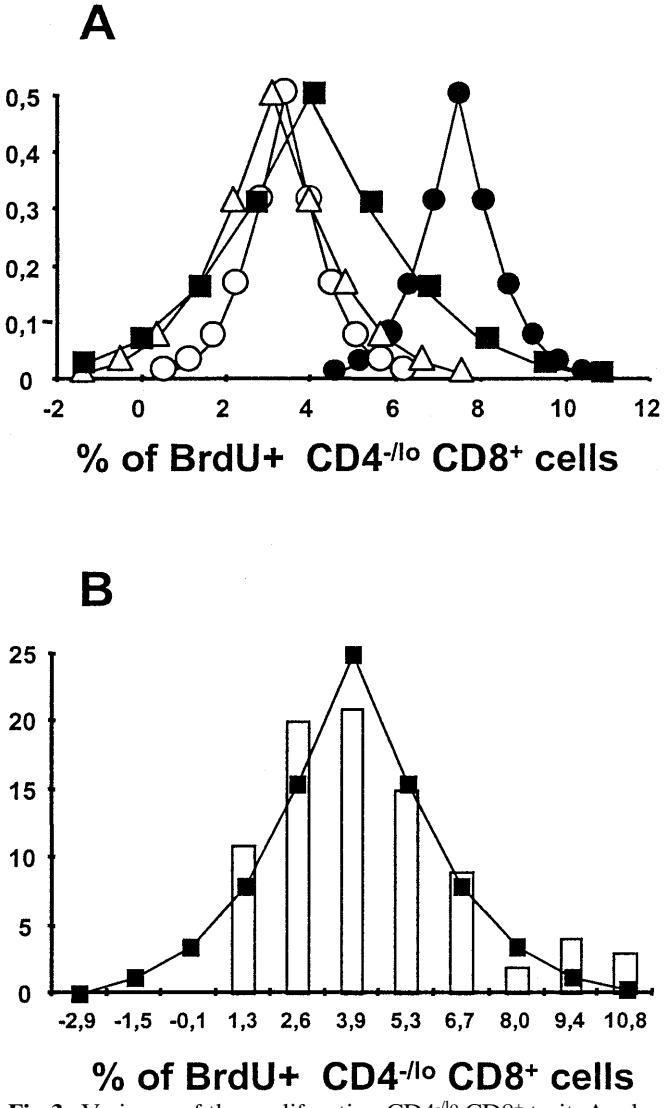

Fig. 3. Variance of the proliferation $CD4^{-/lo}$ $CD8^+$ trait. Analysis of the $CD4^{-/lo}$ $CD8^+$ trait in NOD (○), C57BL/6 (●), F1(C57BL/6XNOD) (△) and F2(C57BL/6XNOD) (■) female mice. The trait was measured in each mouse by the proportion of $CD4^{-/lo}$ $CD8^+$ cells out of the thymocytes incorporating BrdU. **A** Predicted *t*-distribution curves for the $CD4^{-/lo}$ $CD8^+$ trait based on the analysis of 14 NOD, 10 C57BL/6, 8 F1(C57BL/6XNOD) and 87 F2(C57BL/6XNOD) females. **B** Observed frequency distribution in the 87 F2(C57BL/6XNOD) females genotyped in this study is indicated by bars and the predicted distribution curve is superimposed

values to high trait values along the F2 progeny, indicating that the genetic factors controlling the trait were segregating in this cross (Fig. 3). An estimation of the non-genetic variance in the F2 progeny (25) ascribed 80 % of the trait variance to genetic factors.

Defective $CD4^{-/lo}$ $CD8^+$proliferation is linked to the Idd6 locus. Next we tested whether the observed NOD trait was genetically linked to any of the main diabetes susceptibility loci defined in crosses between NOD and C57BL/6 mice. The F2 progeny was analysed for the co-segregation of low proliferation in $CD4^{-/lo}$ $CD8^+$ cells with genetic markers linked to *Idd* susceptibility loci on chromosomes 1, 3, 4, 6, 7, 9, 11, 14 and 17. Genetic association was tested in contingency tables to determine which of these chromosomal regions were linked to the low proliferation phenotype. The F2 mice were classified for the $CD4^{-/lo}$ $CD8^+$ proliferation trait according to a threshold that corresponds to the intermediate value between the averages of the parental strains (Fig. 3). Mice were then scored as NOD-like if they had a trait value below this threshold (< 5.4 %) and as C57BL/6-like if above. Using the chi square tests of association, we found this trait to be linked to several markers on chromosome 6, mapping close to the *Idd6* lo-

Table 3. Association of the proliferation CD $4^{-/lo}$ 8^{+} trait to microsatellite markers in chromosome 6

θ	Marker	Genotype	Nod-like	C57BL/6-like	chi square; 2df (*p* value)
		nn	20	2	
	D6Mit184	nb	35	11	4. 4
0.123	*n* = 87	bb	12	7	
		nn	25	3	
	D6Mit9	nb	33	8	7.6
0.091	*n* = 84	bb	8	7	
		nn	21	1	
	D6Mit64	nb	34	9	8.4
0.127	*n* = 83	bb	9	8	
		nn	21	1	
	D6Mit218	nb	32	9	9.1
0.088	*n* = 86	bb	10	8	
		nn	21	0	
	D6Mit194	nb	35	12	11.0
0.063	*n* = 87	bb	10	8	(0.004)
		nn	21	0	
	D6Mit198	nb	37	10	15.8
0.039	*n* = 87	bb	9	10	(0.0004)
		nn	20	2	
	D6Mit57	nb		8	14.1
0.006	*n* = 87	bb	8	10	(0.0008)
		nn	20	2	
	D6Mit14	nb	40	8	15.8
0.006	*n* = 87	bb	7	10	(0.0004)
		nn	19	2	
	D6Mit15	nb	41	8	15.7
0.011	*n* = 87	bb	7	10	(0.0004)
		nn	21	2	
	D6Mit304	nb	39	8	15.9
	n = 87	bb	7	10	(0.0004)

Results of chi square tests (2 degrees of freedom-df) and the corresponding *p* values are listed. Marker order and recombination fractions (θ) were calculated using Mapmaker software [22]. Genotypes: nn, NOD homozygote; nb, heterozygote; bb, C57BL/6 homozygote

cus [26]). The association reached the highest significance value ($p = 0.0004$) with the marker D6Mit14 (Table 3). No significant association was found with markers closely linked to *Idd* loci mapping on the other chromosomes.

To further define the contribution of the linked region on chromosome 6, we did a QTL analysis by scanning chromosome 6 for loci controlling thymocyte proliferation using the Mapmaker/QTL software [27]. The LOD score values peaked in the same region of chromosome 6 where association was found (Fig. 4), and reached a maximum close to the marker D6Mit15 (LOD = 5.36). This locus, mapping closely to *Idd6*, accounts for 24.7 % of the phenotype variance in the F2 progeny and the NOD allele is likely to dominantly confer the proliferation impairment of immature $CD4^{-/lo}$ $CD8^{+}$ thymocytes. The dominant action of this QTL contrasts with the behaviour of the Idd6 locus believed to be recessive. We used an F2 intercross that allowed us to analyse the B6 resistant allele in the homozygous state and we concluded that in the heterozygous state the NOD allele was dominant (Fig. 4) with reduced penetrance (Table 3). In contrast, the Idd6 locus was described in the context of a genetic backcross in which all Idd resistance alleles appear in the heterozygous state [26]. In such a situation it is difficult to distinguish between a recessive mode of action and a dominant mode with reduced penetrance.

Discussion

In the normal process of thymic T-cell development, the transition of thymocytes from the DN to the DP stage has been associated with cell proliferation [14, 17]. We found that immature thymocytes from the NOD mouse have low cellular expansion when the thymus is depleted of DP cells and that the replenishment of the DP compartment exhibits slow kinetics. The observed slow kinetics of the NOD thymus replenishment correlated with a low number of proliferating cells, particularly in the immature $CD4^{-/lo}$ $CD8^{+}$ and DP populations.

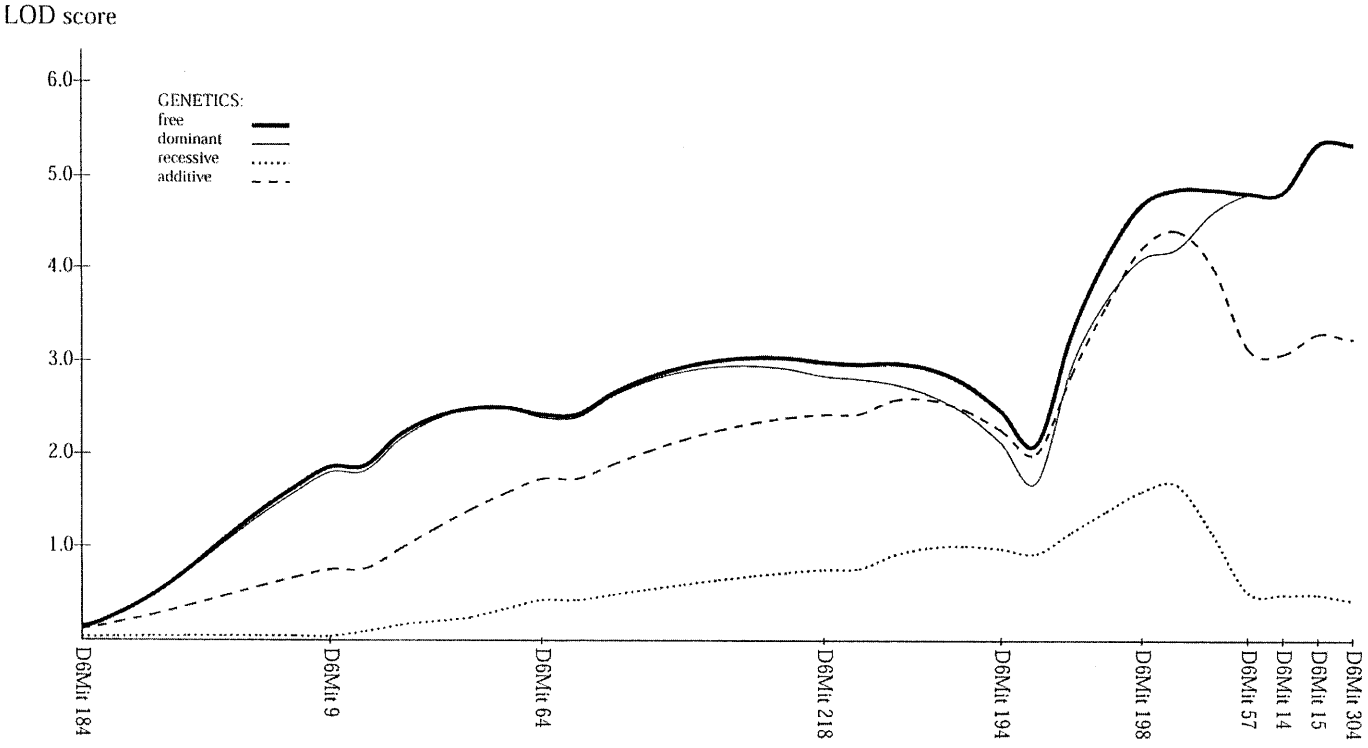

Fig. 4. Quantitative trait locus analysis of the low proliferation of immature thymocytes in the F2 intercross. Plots were generated by QTL 1.1 software [23]. The LOD score curve along chromosome 6 represents the maximum likelihood estimates for the presence of a QTL at each point of the analysed region [22]. Plotted lines show LOD scores over the analysed area of chromosome 6 and the fitness of the NOD allele to particular models of gene action

The $CD4^{-/lo}$ $CD8^+$ thymocyte population has been previously identified as a discrete differentiation stage [28]. Progression into this stage can be enhanced by anti- CD3 antibodies and by transgenic expression of Erg-1, a zinc-finger transcription factor belonging to the immediate-early genes [29]. Inhibition of $CD4^{-/lo}$ $CD8^+$ thymocyte proliferation can be induced by TCR signalling [28] or by down-modulation of the glucocorticoid receptor [30]. These findings support the model of dual antagonism which proposes that activation signals delivered via the TCR complex can inhibit glucocorticoid induced cell death [31, 32] and conversely, that activation of the glucocorticoid receptor can modulate TCR-mediated cell death [33]. In this context, the low proliferation observed in the immature NOD thymocytes could reflect an inhibition of proliferation by signalling through the TCR. Alternatively, this trait could represent a decrease in the intrinsic rate of proliferation within this population.

Genetic mapping identified a locus that controls the proportion of the proliferating $CD4^{-/lo}$ $CD8^+$ thymocytes. This locus is located on the distal region of chromosome 6 and controls 24.7% of the $CD4^{-/lo}$ $CD8^+$ proliferation trait. Although it is not proven here that this locus represents the Idd6 locus, this genetic study shows that $CD4^{-/lo}$ $CD8^+$ proliferation trait is closely linked to the *Idd6* susceptibility region. The identified locus controls 24.7% of the $CD4^{-/lo}$ $CD8^+$ proliferation trait. There was no significant association of this trait to markers reported to be linked to the other *Idd* loci.

This study does not provide a direct correlation of the thymocyte proliferation phenotype with diabetes. Nevertheless, the observed linkage to *Idd6* locus suggests that a susceptibility locus in Idd6 region could mediate its effect on diabetes pathogenesis, through an impaired proliferation of NOD thymocytes during the transition from DN to DP thymocytes. We have reported that resistance of immature NOD thymocytes to glucocorticoid-induced apoptosis maps to the same *Idd6* region [9]. This locus could possibly constitute a genetic factor favouring inhibition of proliferation and increasing the resistance to apoptosis by glucocorticoids in cells undergoing selection in the thymus. As discussed above, signals delivered by the TCR lead both to proliferation inhibition and to apoptosis resistance in immature thymocytes. Therefore, the Idd6 region could contain a genetic factor that is concurrent with the effects of TCR signalling on the proliferation and apoptosis of immature thymocyte. Such a genetic factor could alter the expansion of the TCR repertoire in the immature compartments and would contribute to rescuing an altered repertoire of TCR specificities during intra-thymic T-cell selection.

Acknowledgements. We wish to thank Dr. E. Lander for making the Mapmaker/EXP 3.0 software package and manuals available to us. This work was supported by grants from the Swedish Medical Research Council and the EU commission.

References

1. Makino S, Kunimoto K, Muraoka Y, Mizushima Y, Katagiri K,Tochino Y (1980) Breeding of a non obese, diabetic strain of mice. Jikken Dobutsu 29: 1–13
2. Podolin PL, Denny P, Lord CJ et al. (1997) Congenic mapping of the insulin-dependent diabetes (Idd) gene, Idd10, localizes two genes mediating the Idd10 effect and eliminates the candidate Fcgr1. J Immunol 159: 1835–1143
3. Ikegami H, Ogihara T (1996) Genetics of insulin-dependent diabetes mellitus. Endocr J 43: 605–613
4. Podolin PL, Denny P, Armitage N et al. (1998) Localization of two insulin-dependent diabetes (Idd) genes to the Idd10 region on mouse chromosome 3. Mamm Genome 9: 283–286
5. Vyse TJ, Todd JA (1996) Genetic analysis of autoimmune disease. *Cell* 85: 311–318
6. Acha-Orbea H, McDevitt HO (1987) The first external domain of the nonobese diabetic mouse class II I-A beta chain is unique. Proc Natl Acad Sci U S A 84: 2435–2439
7. Leijon K, Hammarstrom B, Holmberg D (1994) Non obese diabetic (NOD) mice display enhanced immune responses and prolonged survival of lymphoid cells. Int Immunol 6: 339–345
8. Bergman M-L, Cilio CM, Penha-Goncalves C et al. (2001) CTLA-4-/- Mice diplay T cell-apoptosis resistance resembling that ascribed to autoimmune-prone non-obese diabetic (NOD) mice. J Autoimmun 16: 105–113
9. Penha Goncalves C, Leijon K, Persson L, Holmberg, D (1995) Type 1 diabetes and the control of dexamethazone-induced apoptosis in mice maps to the same region on chromosome 6. Genomics 28: 398–404
10. Zipris D, Lazarus AH, Crow AR, Hadzija M, Delovitch TL (1991). Defective thymic T cell activation by concanavalin A and anti-CD3 in autoimmune nonobese diabetic mice. Evidence for thymic T cell anergy that correlates with the onset of insulitis. J Immunol 146: 3763–3771
11. Gill BM, Jaramillo A, Ma L, Laupland KB, Delovitch TL (1995) Genetic linkage of thymic T-cell proliferative unresponsiveness to mouse chromosome 11 in NOD mice. A possible role for chemokine genes. Diabetes 44: 614–619
12. Fischer A, Malissen B (1998) Natural and engineered disorders of lymphocyte development. Science 280: 237–243
13. Zuniga Pflucker JC, Lenardo MJ (1996) Regulation of thymocyte development from immature progenitors. Curr Opin Immunol 8: 215–224
14. Penit C, Lucas B, Vasseur F (1995) Cell expansion and growth arrest phases during the transition from precursor (CD4–8-) to immature (CD4 + 8 +) thymocytes in normal and genetically modified mice. J Immunol 154: 5103–5113
15. Godfrey DI, Kennedy J, Suda T, Zlotnik A (1993) A developmental pathway involving four phenotypically and functionally distinct subsets of CD3-CD4-CD8- triple-negative adult mouse thymocytes defined by CD44 and CD25 expression. J Immunol 150: 4244–4252
16. Fehling HJ, von Boehmer H (1997) Early alpha beta T cell development in the thymus of normal and genetically altered mice. Curr Opin Immunol 9: 263–275
17. Falk I, Biro J, Kohler H, Eichmann K (1996) Proliferation kinetics associated with T cell receptor-beta chain selection of fetal murine thymocytes. J Exp Med 184: 2327–2339
18. Lucas B, Vasseur F, Penit C (1993) Normal sequence of phenotypic transitions in one cohort of 5-bromo-2'-deoxyuridine-pulse-labeled thymocytes. Correlation with T cell receptor expression. J Immunol 151: 4574–4582
19. Surh CD, Sprent J (1994) T-cell apoptosis detected in situ during positive and negative selection in the thymus. Nature 372: 100–103
20. Penit C, Vasseur F, Papiernik M (1988) In vivo dynamics of CD4–8- thymocytes. Proliferation, renewal and differentiation of different cell subsets studied by DNA biosynthetic labeling and surface antigen detection. Eur J Immunol 18: 1343–1350
21. Tough DF, Sprent J (1994) Turnover of naive- and memory-phenotype T cells. J Exp Med 179: 1127–1135
22. Love JM, Knight AM, McAleer MA, Todd JA (1990) Towards construction of a high resolution map of the mouse genome using PCR-analysed microsatellites. Nucleic Acids Res 18: 4123–4130
23. Lander ES, Green P, Abrahamson J, Barlow A, Daly MJ, Lincoln SE, Newburg L (1987) MAPMAKER: an interactive computer package for constructing primary genetic linkage maps of experimental and natural populations. Genomics 1: 174–181
24. Paterson AH, Lander ES, Hewitt JD, Peterson S, Lincoln SE, Tanksley SD (1988) Resolution of quantitative traits into Mendelian factors by using a complete linkage map of restriction fragment length polymorphisms. Nature 335: 721–726
25. Paterson AH, Damon S, Hewitt JD et al. (1991) Mendelian factors underlying quantitative traits in tomato: comparison across species, generations, and environments. Genetics 127: 181–197
26. Ghosh S, Palmer SM, Rodrigues NR et al. (1993) Polygenic control of autoimmune diabetes in nonobese diabetic mice. Nat Genet 4: 404–409
27. Lander ES, Botstein D (1989) Mapping mendelian factors underlying quantitative traits using RFLP linkage maps [published erratum appears in Genetics 1994 Feb: 136: 705]. Genetics 121: 185–199
28. Takahama Y, Shores EW, Singer A (1992) Negative selection of precursor thymocytes before their differentiation into CD4 + CD8 + cells. Science 258: 653–656
29. Miyazaki T (1997) Two distinct steps during thymocyte maturation from CD4-CD8- to CD4 + CD8 + distinguished in the early growth response (Egr)-1 transgenic mice with a recombinase-activating gene-deficient background. J Exp Med 186: 877–885
30. King LB, Vacchio MS, Dixon K, Hunziker R, Margulies DH, Ashwell JD (1995) A targeted glucocorticoid receptor antisense transgene increases thymocyte apoptosis and alters thymocyte development. Immunity 3: 647–656
31. Iwata M, Hanaoka S, Sato K (1991) Rescue of thymocytes and T cell hybridomas from glucocorticoid-induced apoptosis by stimulation via the T cell receptor/CD3 complex: a possible in vitro model for positive selection of the T cell repertoire. Eur J Immunol 21: 643–648
32. Zaitseva MB, Mojcik CF, Salomon DR, Shevach EM, Golding H (1998) Co-ligation of alpha4beta1 integrin and TCR rescues human thymocytes from steroid-induced apoptosis. Int Immunol 10: 1551–1561
33. Ashwell JD, King LB, Vacchio MS (1996) Cross-talk between the T cell antigen receptor and the glucocorticoid receptor regulates thymocyte development. Stem Cells 14: 490–500